

Prestressed Concrete Inverted Tee Beams with CFRP for Building Structures

Herish A. Hussein¹ and Zia Razzaq²

¹ Old Dominion University

Received: 10 December 2016 Accepted: 2 January 2017 Published: 15 January 2017

Abstract

Presented herein is the outcome of a study of prestressed concrete inverted tee beams with carbon fiber reinforced polymer (CFRP) sheets for possible use in building structures. To determine an effective approach for the use of CFRP, nine different retrofitting schemes are investigated for a prestressed beam under quasi-static distributed load to increase flexural strength. The theoretical analysis is based on coupling moment-curvature relations with a central finitedifference formulation. Three different thicknesses of CFRP sheets are studied in both tension and compression and effective retrofitting schemes are identified.

Index terms— CFRP retrofitting, inverted tee beam, prestressed.

1 Introduction

he effectiveness of CFRP retrofitting when used only in tension zone of prestressed concrete beams has been reported in the past [1][2][3][4][5][6][7][8]. The use of CFRP is beneficial due to its high strength, light weight, non-corrosive nature, and easy installation. [9] Hussein and Razzaq [10] have previously published a study of prestressed concrete box girders with CFRP retrofitting in both tension and compression for use in highway bridges. Presented in this paper is a study of the effectiveness of CFRP sheets in increasing strength and decreasing deflection when used not only in tension but also in compression, or in both tension and compression regions for prestressed concrete inverted tee beams in buildings.

2 II.

3 Problem Statement

A prestressed concrete inverted tee beam is shown in Figure ?? carrying a distributed load in addition to its self-weight of 0.45 kips/ft. Figure ??a shows the inverted tee beam cross section without retrofitting. Figures ??b through 2d show the beam cross section retrofitted with single CFRP sheet in tension only, compression only, and simultaneously in both tension and compression, respectively. The CFRP sheet is 1/16 in. thick with a constant width of 11in. The same retrofitting approaches are repeated with doubling and tripling the CFRP sheets as shown in Figures ??e-2g and 2h-2j, respectively. Each beam has eight 7-wire ASTM Grade 270 ½ diameter strands in one row as shown.

The following non-linear stress-strain relationship for concrete given by Lin and Burns [11] is adopted for the present study: (1) where is the ultimate compression strength at concrete strain

The concrete use d in this study has an ultimate strength of 8 ksi and a Young's Modulus of 5148 ksi. Furthermore, the CFRP sheet used has an ultimate tensile rupture strength of 260 ksi and a Young's Modulus of 22000 ksi. The stress-strain relation for CFRP in compression is nearly the same as in tension. An elastic-plastic stress-strain relation is adopted for prestressing steel. The problem addressed in this paper is the identification of effective CFRP retrofitting schemes that can practically be utilized for prestressed concrete inverted tee beams in building structures. This is achieved by first developing nonlinear moment-curvature (M-?) relations for cross

sections shown in Figure ?? followed by the formulation of a numerical scheme to predict the load-deflection response of the beam shown in Figure ?? up to collapse.

4 III.

5 Nonlinear Solution Procedure

The prestressing strands have a prestress force of 160 kips after prestress losses. Figure 3 shows a typical prestressed beam and strain distribution as well as the associated concrete compressive stress distribution and internal force resultants. The resultant forces are C_c , T_{ps} , and T_{CFRP} representing, respectively, concrete compression force, prestressing force, and CFRP tensile force. The equation of the resultant force on the compressed concrete and its distance X from the neutral axis are given by [11]:

(2) (3) where: b = cross-sectional width at the top, c = neutral axis distance as shown in Figure 3b, and ϕ = curvature.

Various loading stages are used to generate the moment-curvature relations. The loading stages are zero external moment, zero strain in concrete at the center of the strands, cracking moment, and the concrete strain reaching 0.001, 0.002, 0.00248, and 0.003 in./in. Elastic bending stress and axial stress equations are used for analysis until the cracking moment is achieved. For the non-linear range, force equilibrium is satisfied after assuming top fiber strain and then iteratively finding the neutral axis location that is, the distance c . The moment and curvature values are then calculated and used to generate the moment-curvature relations for each beam section shown in Figure ?. For the retrofitting schemes with single, double, and triple CFRP sheets in tension, compression, and in both tension and compression, the moment-curvature ($M-\phi$) relationships developed are presented in Figures 4,5, and 6, respectively. Next, the moment-curvature relationships are curve-fitted using Excel for each of the beam sections shown in Figure ?. For all of the non-retrofitted and retrofitted schemes, the following equation is established for the materially linear range:

For the nonlinear portion, the following $M-\phi$ equations are developed for sections shown in Figures ??a through 2j, respectively:

It should be noted that the last point on the $M-\phi$ relations for beam sections 2c, 2f, and 2i are excluded in the above $M-\phi$ equations. However, the excluded points are separately included when determining the load-deflection relations.

6 Global Journal of Researches in Engineering () Volume XVII Issue III Version

$I = 2 \text{ Year } 2017 \text{ E C } c = b \times c^2 \times \delta \text{ ??? } \delta \text{ ??? } \text{ ??? } \times \text{ ??? } (1 - \text{ ??? } \times c \text{ ??? }) X = c(\text{ ??? } \text{ ??? } \text{ ??? } \times c \text{ ??? } \text{ ??? } \text{ ??? } 4$

$\text{ ??? } \times c) \text{ ??? } = (0.0005M -1.2) \times 10^{-5} \text{(4)}$

$\text{ ??? } a = (0.008 \times \text{ ??? } 0.001 \text{ ??? }) \times 10^{-5}$

$(5) \text{ ??? } b = (0.0000006M^2 -0.005M + 9.54) \times 10^{-5} \text{(6) } c = (0.007 \times \text{ ??? } 0.001 \text{ ??? }) \times 10^{-5} \text{(7) } d = (0.0057M - 32.56) \times 10^{-5} \text{(8)}$

$\text{ ??? } e = (0.0000002M^2 -0.0003M -2.61) \times 10^{-5} \text{(9)}$

$\text{ ??? } f = (0.0038 \times \text{ ??? } 0.001 \text{ ??? }) \times 10^{-5} \text{(10) } g = (0.0000001M^2 + 0.001M -4.6) \times 10^{-5} \text{(11) } h = (0.0000001M^2 + 0.0006M -4.26) \times 10^{-5} \text{(12)}$

$\text{ ??? } i = (0.0023 \times \text{ ??? } 0.001 \text{ ??? }) \times 10^{-5}$

$(13) \text{ ??? } j = (0.0026M -14.5) \times 10^{-5} \text{(14)}$ To determine the load-deflection relation for each scheme, the $M-\phi$ relations are coupled with a central finite-difference algorithm similar to that used by the authors [10]. For the present study, the beam is divided into ten equal segments ($h=L/10$), and the curvature at any given node i along the beam length is expressed as [12]: $\phi_i = \text{ ??? } \phi_{i-1} + \text{ ??? } \phi_{i+1}$ where: (a) (b) (c) (d) (e) (f) (g) (h) (i) (j)

V_i = deflection at beam node i .

To calculate the external moment value at any node for various applied loads, the following equation is used: (16) where z is the beam longitudinal axis.

The nonlinear solution algorithm predicting the beam response are as follows: 1. Specify beam length L , cross-sectional dimensions, and material properties for concrete, prestressing strands, and CFRP sheets. 2. Divide the beam into N equal segments along the longitudinal axis associated with node numbers $i = 1, 2, 3, \dots, (N+1)$ over the domain $0 \leq z \leq L$. 3. Specify external load $w = w_1$. 4. Determine M_z using Equation 16 at all nodal locations. 5. With M_z from step four, determine ϕ using the applicable Equation 4-14. 6. Using Equation 15, generate the following matrix equation to determine nodal deflections, V_i : $[Q]\{V_i\} = \{F_i\}$ (17)

7. Solve Equation 17 for the nodal deflection vector $\{V_i\}$.

8. Increase w to w_2 that is, set $w_2 = w_1 + \Delta w$ and go to step 4. 9. Repeat until the load-carrying capacity is reached corresponding to the collapse condition. Using the above algorithm, load versus midspan deflection, V_6 , are predicted and are presented in Figures 7, 8 and 9 for CFRP retrofitted beam sections of 2b-d, 2e-2g, and 2h-2j respectively.

IV.

7 Numerical Study

99

100 Figure ??0 compares the maximum moment versus CFRP thickness relations when CFRP is used in tension only
 101 to the schemes in which CFRP is used simultaneously in both tension and compression. A comparison of the two
 102 curves in this figure reveals that using CFRP in both tension and compression has a greater effect on increasing
 103 the moment capacity compared to the scheme involving retrofitting as the tensile side only.

104 For the presented study, Table 1 presents a summary of the various retrofitting schemes. Presented in this
 105 table are the neutral axis location c , the collapse load w_{max} , and the increase in w_{max} , w^* .

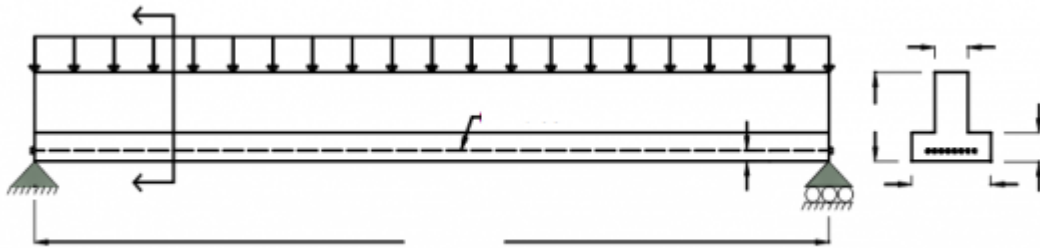
106 As can be seen from Table 1, the most effective retrofitting scheme is when three CFRP sheets are
 107 simultaneously used in both tension and compression. This scheme (section 2j) resulted in a strength of 2.22
 108 times that obtained with the reference beam (section 2a). The remaining retrofitting schemes are found to be
 109 from 1.02 to 1.92 times stronger than the reference beam. $\sigma_i = (\sigma_{i-1} - \sigma_{i+1}) / (V_i - V_{i+1})$

8 Conclusions

110

111 Based on the various CFRP retrofitting schemes studied in this paper, the following principal conclusions are
 112 drawn: 1. Developing upon the desired degree of increase in the load-carrying capacity of a prestressed inverted
 113 tee beam, are more of the retrofitting schemes considered in this paper can be utilized. 2. The simultaneous use
 114 of CFRP retrofitting on both tension and compression is the most effective of the retrofitting schemes considered
 115 in this paper.

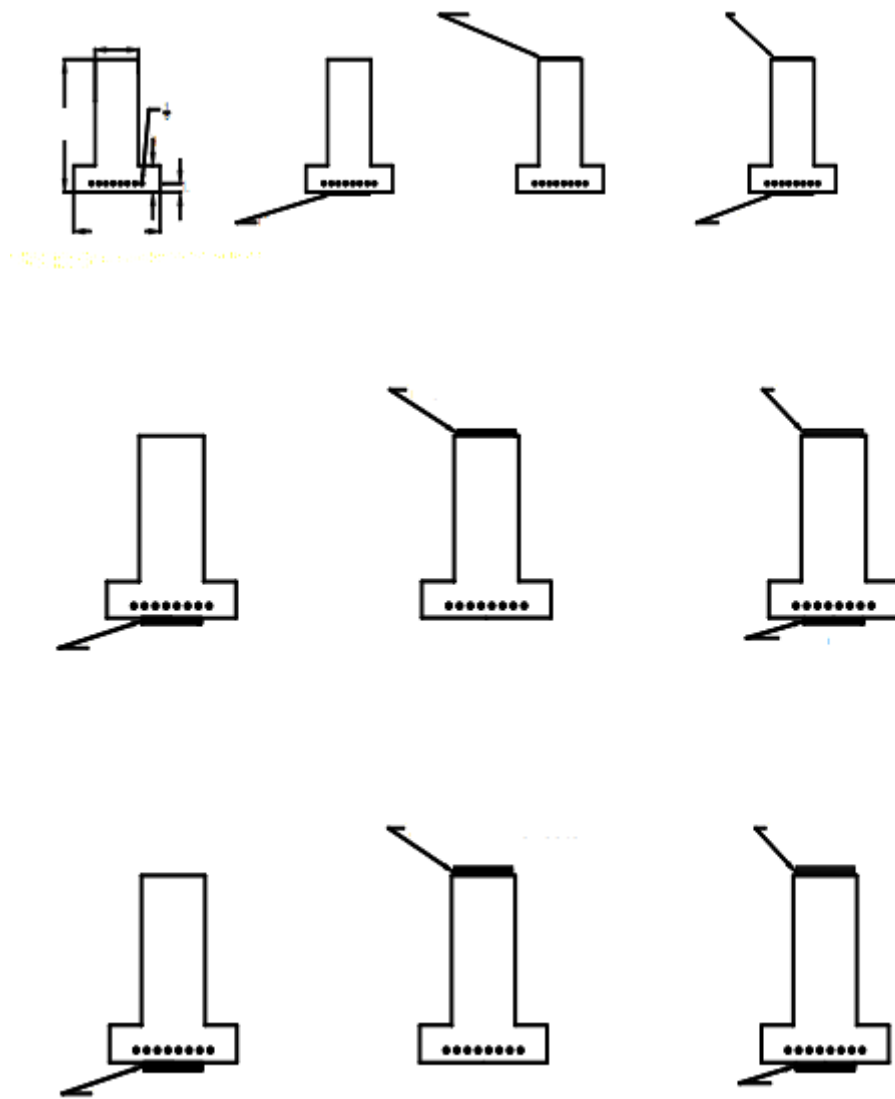
116 The results presented in this study can possibly be implemented in practical CFRP retrofitting issues, related
 to prestressed inverted tee beams in building structures. ¹



12

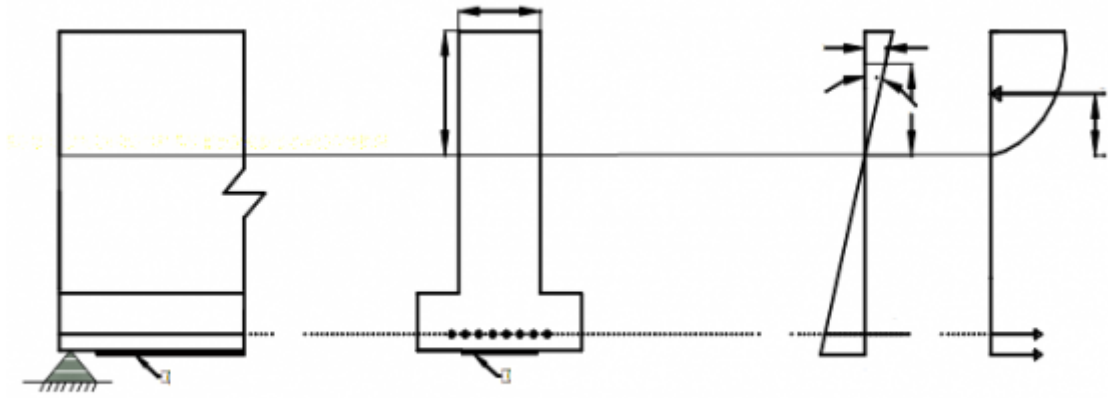
Figure 1: Figure 1 :Figure 2 :

117



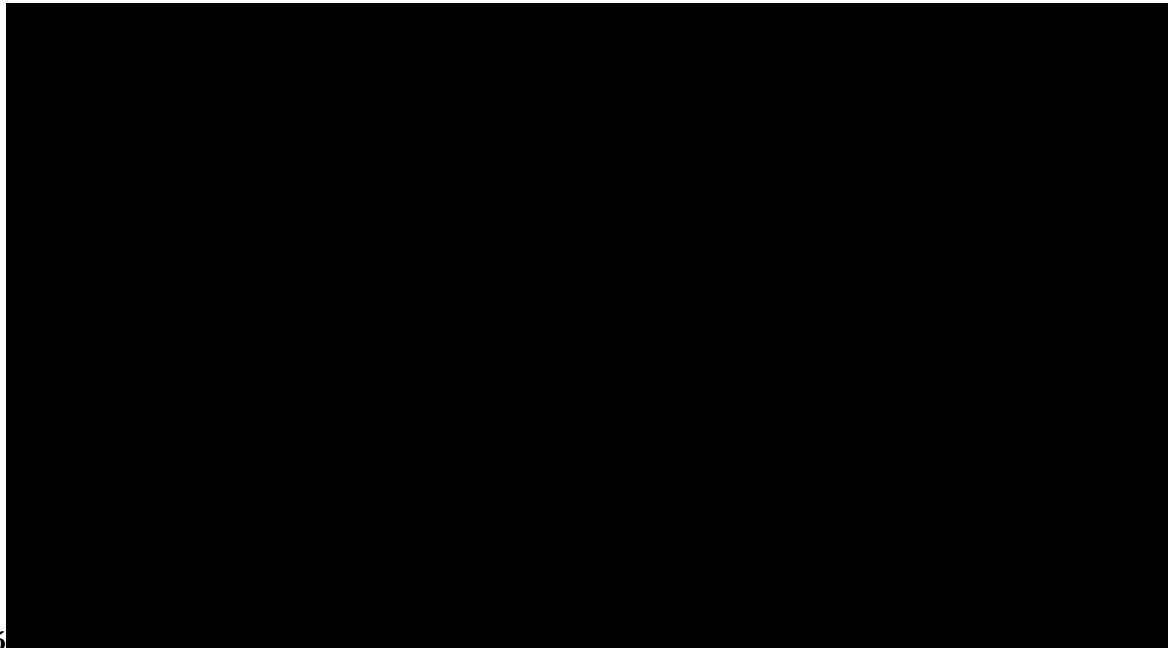
3

Figure 2: Figure 3 :



4

Figure 3: Figure 4 :



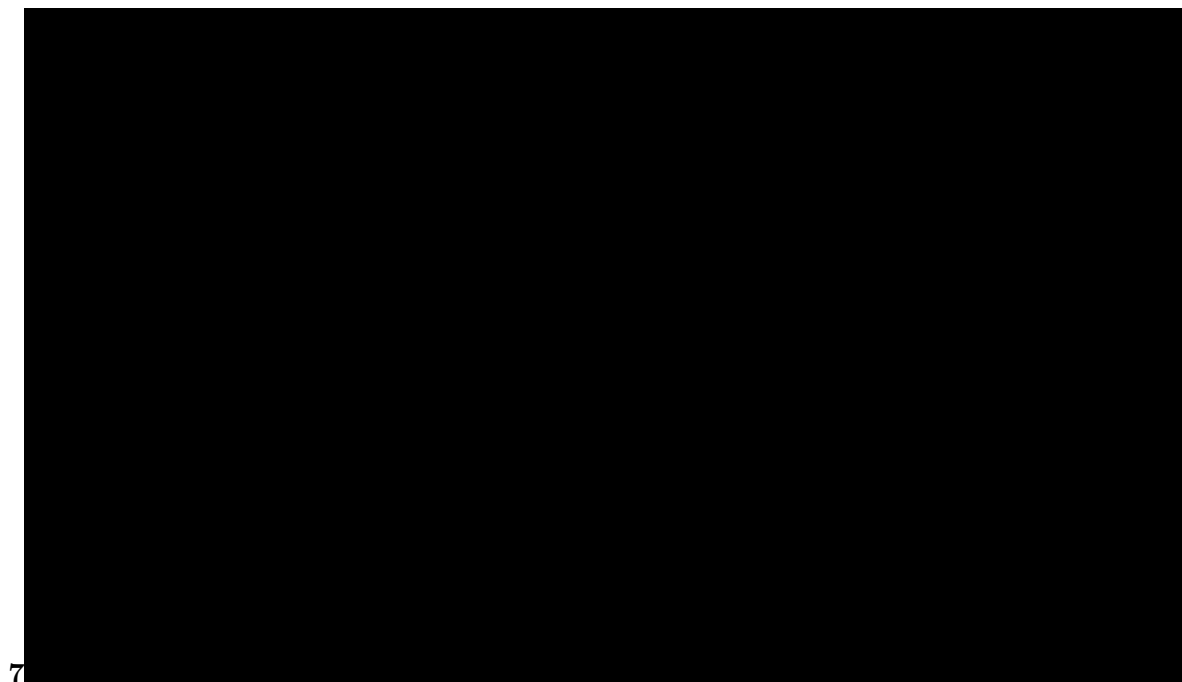
5

Figure 4: PrestressedFigure 5 :



6

Figure 5: Figure 6 :



7

Figure 6: Figure 7 :

1

Year 2017

7

Global Journal of Researches in Engineering () Volume XVII Issue III Version I

E

Figure 7: Table 1 :

-
- 118 [Composites Part B: Engineering ()] , *Composites Part B: Engineering* 2008. 39 p. .
- 119 [Hussein and Razzaq ()] ‘CFRP Retrofitting Schemes for Prestressed Concrete Box Beams for Highway Bridges’
120 H A Hussein , Z Razzaq . *Global Journal of Research In Engineering* 2017.
- 121 [Lin and Burns ()] *Design of prestressed concrete structures*, T Y Lin , N H Burns . 1981.
- 122 [Kim et al. ()] ‘Ductility and cracking behavior of prestressed concrete beams strengthened with prestressed
123 CFRP sheets’. Y J Kim , C Shi , M F Green . *Journal of composites for construction* 2008. 12 p. .
- 124 [Galal and Sekar] *E Prestressed Concrete Inverted Tee Beams with Cfrp for Building Structures 8000 most*
125 *effective retrofitting schemes investigated herein result in a very significant reduction in the beam deflection*,
126 K Galal , M Sekar . (Rehabilitation of RC inverted-T girders using anchored CFRP sheets)
- 127 [Deifalla and Ghobarah ()] ‘Effectiveness of the extended CFRP U-jacket for strengthening of RCT beams under
128 combined torsion and shear’. A Deifalla , Ghobarah . *The 7th international conference on multi-purpose high*
129 *rise towers and tall buildings*, (Dubai, UA) 2005.
- 130 [Aram et al. ()] ‘Effects of gradually anchored prestressed CFRP strips bonded on prestressed concrete beams’.
131 M Reza Aram , C Czaderski , M Motavalli . *Journal of Composites for Construction* 2008. 12 p. .
- 132 [Engineering (2017)] Prince Engineering . [http://www.build-on-prince.com/carbon-fiber.html#](http://www.build-on-prince.com/carbon-fiber.html#sthash.zXRHe178.dpbs)
133 [sthash.zXRHe178.dpbs](http://www.build-on-prince.com/carbon-fiber.html#sthash.zXRHe178.dpbs) *Carbon Fiber used in Fiber Reinforced Plastic Available*, 2017. September 25.
- 134 [Kim et al. ()] ‘Flexural behaviour of reinforced or prestressed concrete beams including strengthening with
135 prestressed carbon fibre reinforced polymer sheets: application of a fracture mechanics approach’. Y J Kim ,
136 M F Green , R G Wight . *Canadian Journal of Civil Engineering* 2007. 34 p. .
- 137 [El-Hacha et al. ()] ‘Prestressed carbon fiber reinforced polymer sheets for strengthening concrete beams at room
138 and low temperatures’. R El-Hacha , R G Wight , M F Green . *Journal of Composites for Construction* 2004.
139 8 p. .
- 140 [Bennitz et al. ()] ‘Reinforced concrete T-beams externally prestressed with unbonded carbon fiber-reinforced
141 polymer tendons’. A Bennitz , J W Schmidt , J Nilimaa , B Täljsten , P Goltermann , D L Ravn . *ACI*
142 *Structural Journal* 2012. 109 p. 521.
- 143 [Burningham et al. ()] ‘Repair of prestressed concrete beams with damaged steel tendons using post-tensioned
144 carbon fiber-reinforced polymer rods’. A Burningham , C P Pantelides , L D Reaveley . *ACI Structural Journal*
145 2014. 111 p. 387.
- 146 [Mitchell and Griffiths ()] *The finite difference method in partial differential equations*, A R Mitchell , D F
147 Griffiths . 1980. John Wiley.